

## Surface modification of cellulose fibers from oil palm empty fruit bunches for heavy metal ion sorption and diesel desulphurization

M.S. Nazir<sup>a,b</sup>, H. Ajab<sup>c</sup>, M.R. Raza<sup>d</sup>, M.A. Abdullah<sup>e,\*</sup>

<sup>a</sup>Department of Chemical Engineering, Universiti Teknologi PETRONAS, 32610 Seri Iskandar, Perak, Malaysia, email: shahid.nazir@ciitlahore.edu.pk, biochemistsn@gmail.com (M.S. Nazir),

<sup>b</sup>Present address: Department of Chemistry, COMSATS Institute of Information Technology, Lahore, 54000, Punjab, Pakistan,

<sup>c</sup>Department of Chemistry, COMSATS Institute of Information Technology, Abbottabad, 22060, Pakistan, email: humaajab@ciit.net.pk, humaajab@hotmail.com (H. Ajab),

<sup>d</sup>Department of Mechanical Engineering, COMSATS Institute of Information Technology Sahiwal, 57000 Pakistan, email: rafirazamalik@ciitsahiwal.edu.pk, rafirazamalik@gmail.com (M.R. Raza),

<sup>e</sup>Institute of Marine Biotechnology, Universiti Malaysia Terengganu, 21030 Kuala Nerus, Terengganu, Malaysia, Tel. +609-6683104/3661, Fax +609-6683105, email: azmuddin@umt.edu.my, joule1602@gmail.com (M.A. Abdullah)

Received 25 September 2017; Accepted 7 March 2018

### ABSTRACT

In this study, purely-extracted cellulose from Oil Palm Empty Fruit Bunches (OPEFB) were successfully surface-engineered with acetate (mono-carboxylic), oxalate (di-carboxylic) and ethylene diamine tetra acetic acid (tetracarboxylic group) with different degree of substitution, due to the presence of carboxylic group on the an hydro glucose unit of cellulose. The changes from smooth to rough surface can be attributed to the effects of sodium hydroxide treatment and distribution of carboxylic group. All Fourier transform infrared spectroscopy spectra showed similar peaks suggesting the stability of purely-extracted cellulose structure after treatment. The only difference was the 1730 cm<sup>-1</sup> peak for carboxylic group (C=O) observed in all substituted spectra, but not in the original purely-extracted cellulose. The ultrasonic and autoclave treatments of cellulosic fibers modified (M) with the carboxylic groups showed the highest Pb(II) adsorption from EDTA modified (232.9 and 236.7 mg g<sup>-1</sup>) sorbents. The low Pb (II) ion uptake at pH 4 was attributable to the competition for the active sites with higher concentration of protons, while higher uptake was attained at pH 6 with more abundant hydroxyl ions. The Pb (II) sorption on the surface engineered sorbents followed the pseudo second order kinetics model with  $R^2 = 0.9771$ – $0.9809$ , and best fitted to the Temkin adsorption isotherms. The Pb-loaded modified purely-extracted celluloses were tested for desulphurization of diesel and achieved higher sulphur removal (ppm) from the Pb-Oxalate-modified (300) and Pb-EDTA-modified (350) sorbents as compared to without metal-loaded sorbents (80–110).

**Keywords:** Purely-extracted celluloses; Biosorption; Lead; Adsorption kinetics; Diesel desulphurization

### 1. Introduction

Many methods have been employed for the removal of heavy metals from aqueous solutions such as membrane separation by reverse osmosis or ultra filtration, electro dialysis, ion exchange, chemical precipitation, flocculation or coagulation, electrochemical or chemical oxidation/

reduction and adsorption. These may have low efficiency, high cost, and generate toxic wastes. Adsorption is advantageous because of its fast kinetics with high adsorption capacity and broad spectrum selectivity towards metal ions. Different modified sorbents have been reported for heavy metal ions removal such as polyacrylonitrile-based fiber modified with thiosemicarbazide and polyaniline nano fibers assembled on alginate micro sphere for both Cd (II) and Pb (II) removal [1,2] and polyrhodanine modified

\*Corresponding author.

multi-walled carbon nanotubes for Pb (II) removal from aqueous solution [1]. Amino-magnetic glycidyl methacrylate resins have been developed for the recovery of thorium ions from granite leach liquors [3], surfactant-modified carbon for the removal or detection of Cd (II) and Hg (II) sorption from aqueous solution [4,5], bentonite-based materials for wastewater treatment [6]. Other agro-wastes used as biosorbents for heavy metal ions removal include oil palm wastes and *Ceiba pentandra* [7,8], coconut fiber [9], fir cone powder [10], banana peels [11], groundnut husk [12], date bead carbon activated [13] and sawdust [14]. Chitosan resins have excellent properties (high adsorption capacity for metal ions and dyes, non-toxic, biocompatible and cost effective) for the treatment of various types of pollutants from water and wastewater [15].

Agro-based biopolymer matrices are becoming increasingly important for environmental remediation due to low cost, reusability, biodegradability and having high sorption capacity. As sulphur is one of the major air pollutant produced from refineries, vehicles and fuel combustion, agro based biopolymer may find great potential application in the desulphurization of diesel. Organosulphur compounds such as thiophene, benzothiophene, dibenzothiophene (DBT), and alkylated DBT that exist in products must be treated to reduce the sulphur content from 300 ppm to below 50 ppm to meet the European Union standard [16]. There has been recommendation to reduce the sulphur content of petrol and diesel fuels further to below 50 ppm. Most benefits of sulphur reduction with current production (stoichiometric) of petrol vehicles come at the 10 ppm level, with only marginal benefits at the 30 ppm level. Reducing the sulphur content of diesel from 50 ppm to 10 ppm will enable more active oxidation catalysts to be used while maintaining or reducing sulphur based particulate emissions. This use of more active oxidation catalysts will reduce carbon based PM emissions [17]. Hydro-treatment is a commercially established method for sulphur removal, which involves heating the feedstock with hydrogen fed into a reactor loaded with catalyst [18]. It is the combination of many sub-processes such as hydrode sulphurization (HDS) for sulphur, hydro-dehydrogenation (HDN) for nitrogen, hydro-deoxygenation (HDO) for oxygen, and hydro-demetalization (HDM) for metals [19]. The technology via HDS and direct desulphurization (DDS) pathway can be risky and costly due to high operating conditions and the use of catalysts, and produces  $H_2S$  which is a toxic flue gas.

Desulphurization of hydrocarbon via dispersing metal ions in a matrix structure has been reported, allowing the polar sulphur site of organosulphur to attach to the metal ions. The negatively charged sulphur compounds may interact with the positively charged metal-loaded sorbent. The metal phase is selective to reversible adsorption of sulphur using thiophene and dibenzothiophene as organosulphur compounds [20]. Effective porous lignocellulosic matrix can be developed as a medium for sulphur adsorption [21]. Celluloses extracted from agro-based ligno cellulosic materials and the surface engineered cellulose fibers have potential applications as biosorbents and can be developed for desulphurization of hydrocarbon feedstock such as diesel and motor gasoline. Surface engineering parameters include the types of modifiers, the number of functional groups on cellulosic fibers such as  $-COOH$  that could attract positively

charged heavy metal ions and the sulphur compounds. The  $\beta$ -D-glucopyranose unit is responsible for the elongation of cellulose polymeric chain bearing one primary ( $p^\circ$ )  $-OH$  group and two secondary ( $S^\circ$ )  $-OH$  group. These three  $-OH$  groups are prone to modifications by using variety of functional groups such as (a) acid anhydride including succinic, maleic and propionic acids; (b) acid chloride such as ketone carboxylic group; (c) alkyl chloride including acrylonitrile and  $\beta$ -propiolactone; or (d) monoepoxyoxide and diepoxides and aldehydes [22,23].

The objectives of this study were to develop surface modification of purely extracted celluloses (PECs) with different modifiers (i.e. acetic acid, oxalic acid and EDTA) for heavy metal ion sorption and diesel desulphurization. The characteristics of raw OPEFB and PEC-OPEFB were compared based on FESEM, and FTIR and the degree of substitution was established. The parameters investigated included the contact time, initial concentration and pH. The kinetics and modeling of heavy metal ion sorption was established based on the first order and second order kinetics, the Langmuir, Freundlich and Temkin adsorption isotherms.

## 2. Materials and methods

### 2.1. Materials

Fresh OPEFB samples were collected from the Palm Oil Mill, FELCRA Nasaruddin, Bota, Perak, Malaysia and stored at  $4^\circ C$ . The ACS grade chemicals- n-hexane ( $n-C_6H_{14}$ ), sodium hydroxide (NaOH) (pellet), (30%) hydrogen peroxide ( $H_2O_2$ ) and ethanol ( $C_2H_6O$ ) (99.5%), formic acid ( $CH_2O_2$ ) (96.0%), acetic acid ( $CH_3COOH$ ), oxalic acid ( $COOH$ )<sub>2</sub> and ethylene diamine tetra acetic acid (EDTA) and the commercial grade micro crystalline cellulose (MCC) were purchased from Sigma-Aldrich. The instruments used were Stirring Hot Plate (Fisher Scientific, 1110250SH), 40kHzsonicator (Elma Transsonic T910 DH), autoclave (75X, All American), and deionized water system (Thermo Scientific, TK Japan).

### 2.2. Cellulose extraction

#### 2.2.1. Pre-treatment

Raw fibers were separated from the OPEFB, washed with 1% detergent to remove oil, grease, and suspended particles until the cleaned water turned from dark brown to colorless. The fibers were cut into 10 mm length using a power cutting mill (PULVERISSETTE 25) and further ground to 0.2 mm size using a bench top ring mill (Rocklabs LTD, New Zealand) [24]. Fibers were air dried and used as raw OPEFB.

For treated fibers, samples were dried in an oven (UNB-400, MEMERT) at  $60^\circ C$  for 12 h. Soxhlet extraction was applied to remove wax and oily layer. Ten g of fibers were placed in the cellulose thimble with ethanol as extracting solvent. Temperature was set at  $85^\circ C$  to allow dewaxing of fibers, evaporation and condensation, before being filtered and drained back into the flask. The cycle was repeated several times for 6 h. The dewaxed fibers were then washed with deionized water to remove alcohol traces, before further drying.

### 2.2.2. Sonication-chemical extraction (SONO-CHEM) and autoclave-chemical extraction (AUTO-CHEM)

The dewaxed fibers were further treated by the SONO-CHEM and AUTO-CHEM methods adopted and modified for cellulose extraction as described before [25,26]. The  $\alpha$ -cellulose content of the extracted residue was determined based on the TAPPI test method (T 203 om-88) [27]. The extracted cellulose was determined by Eq. (1):

$$\text{Cellulose}(\%) = \frac{W_{od} - W_{loss}}{W_{od}} \times 100 \quad (1)$$

where  $W_{od}$  (g) is the mass of the oven dried OPEFB before treatment,  $W_{loss}$  (g) is the weight loss after cellulose extraction.

### 2.3. Chemical treatment for surface modification of PECs

PEC-OPEFB hydroxyl groups were regenerated in 70% ethanol at room temperature and 250 rpm stirring speed for 1 h, filtered and washed with deionized water. The PEC-OPEFB was mercerized using standard procedure based on ASTM D 1695 [28], where 100 g of cellulose was suspended in 1 L of 0.1 M NaOH solution for 4 h at room temperature and continuously shaken at 250 rpm. Mercerized PEC-OPEFB (PEC-OPEFB-ONa) was further filtered, washed and dried in an oven. PEC-OPEFB-ONa was treated with 0.1 M acetic acid, oxalic acid and EDTA, with acetic anhydride used as catalyst, and refluxed for 4 h at 100°C. The modified PEC, based on the treatment applied, was given the abbreviation and described in Table 1. These were filtered and washed before characterization and sorption studies.

The degree of substitution (DS) was determined as described earlier [29]. Five of each sample was suspended in NaOH (1 mol L<sup>-1</sup>) for 12 h, filtered and the filtrate was

titrated against the standard H<sub>2</sub>C<sub>2</sub>O<sub>4</sub> (1 mol L<sup>-1</sup>) by using phenolphthalein indicator. The DS was calculated by Eq. (2):

$$DS = \frac{162 \times 20(C_i - C_f)}{1000W - 42 \times 20(C_i - C_f)} \quad (2)$$

where  $C_i$  and  $C_f$  are the concentration of NaOH before and after the treatment of PEC-OPEFB (mol L<sup>-1</sup>),  $W$  is the weight of the sample (g).

### 2.4. Characterization

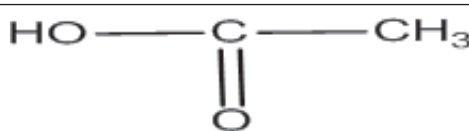
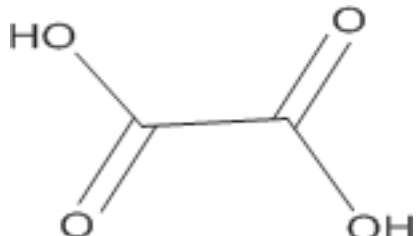

The outer surface of the modified material was characterized by using the FESEM (Zeiss Supra 55VP). One drop of the sample was placed on a carbon tap and allowed to dry for 24 h at room temperature. The samples were then gold coated with the sputtering method to avoid charges and the accelerated voltage was set to 2 kV. The samples were analyzed and morphological changes were recorded at 50.00 kX magnification. The mean diameter was determined based on 10 fibers randomly selected from the image.

The functional group was investigated by FTIR (Spectrum one, Perkin Elmer). Samples were prepared by mixing KBr and cellulose pressed to the disc at 1:10 ratio. The FTIR spectra were produced after fifty times scanning at 4 cm<sup>-1</sup> resolution transmission and the wave number range of 4000 to 450 cm<sup>-1</sup>.

### 2.5. Heavy metal ion sorption

The heavy metal ion stock solutions were prepared by dissolving 1 g of lead nitrate in 1 L deionized water. For batch adsorption studies, one g of each adsorbent was suspended in 100 mL of metal ion working

Table 1  
Grafting groups, modified cellulose and the degree of substitution

Reagent molecule	Formulae	Material	Abbreviation	Degree of substitution
Acetic acid		PEC-OPEFB-Acetate-US	MAcUS	1.95
		PEC-OPEFB-Acetate-Auto	MAcAUTO	1.67
Oxalic acid		PEC-OPEFB-Oxalate-US	MOUS	1.29
		PEC-OPEFB-Oxalate-Auto	MOAUTO	1.18
EDTA		PEC-OPEFB-EDTA-US	MEUS	0.778
		PEC-OPEFB-EDTA-Auto	MEAUTO	0.874

solution in 250 mL Erlenmeyer flask and agitated at 150 rpm (Orbital shaker, Fischer) for different duration over 360 min period and the heavy metal ion concentrations between 100–500 ppm at pH 6 and room temperature ( $25 \pm 1^\circ\text{C}$ ). The pH effect was determined at 100 ppm concentration at 1 g sorbent for 90 min and 150 rpm agitation. The pH variation was adjusted with 0.01 M  $\text{CH}_3\text{COOH}$  and 0.01 M  $\text{NaOH}$  and recorded with pH-meter (pH 510, EUTECH, Instrument). At pH 8, white precipitates of  $\text{Pb}(\text{OH})_2$  were formed which was later dissolved in 1 mL of  $\text{CH}_3\text{COOH}$  before filtration. At the end of each experiment, samples were filtered and the metal ion concentration of the filtrate was analyzed by using Atomic Absorption Spectrometer (AAS, Hitachi Z-5000). Each experiment was performed in triplicate and the mean values were reported.

The amount of metal ion adsorbed at equilibrium,  $q_e$  was calculated by Eq. (3):

$$q_e = \left( \frac{C_i - C_f}{C_i} \right) \times 100 \quad (3)$$

where  $C_i$  ( $\text{mg L}^{-1}$ ) is the initial metal ion concentration of the working solution and  $C_f$  ( $\text{mg L}^{-1}$ ) is the final metal ion concentration at equilibrium.

## 2.6. Kinetics studies

The adsorption kinetics of Pb (II) ions were investigated by two commonly used models:- pseudo-first-order and pseudo-second-order. Model equations were fitted to the experimental data and the values were expressed by the correlation coefficient ( $R^2$ ) which determined the fitness of the model using Microsoft Excel (2007).

### 1.1.1. Pseudo-first-order

The pseudo-first-order rate model of Lagergren [30] is based on the solid capacity and generally expressed as the following equation:

$$\log(q_e - q) = \log q_e - \left( \frac{k_1}{2.303} \right) t \quad (4)$$

where  $q_e$  is the equilibrium concentration of the metal ions adsorbed per unit mass of sorbent ( $\text{mg g}^{-1}$ ),  $q$  is the metal ions adsorbed ( $\text{mg g}^{-1}$ ) at the time  $t$ (s), and  $k_1$  ( $\text{min}^{-1}$ ) is the adsorption rate constant. A straight line is then plotted as  $\log(q_e - q)$  with respect to time ( $t$ ) which gives the slope of  $k_1/2.303$  and  $\log q_e$  as the intercept.

### 1.1.2. Pseudo-second-order

Pseudo-second-order kinetic model in linear form can be expressed by Eq. (5):

$$\frac{t}{q} = \left( \frac{1}{k_2 q_e^2} \right) + \left( \frac{1}{q_e} \right) t \quad (5)$$

$$h = k_2 q_e^2 \quad (6)$$

The plot of  $t/q$  versus  $t$  gives a straight line where  $q_e$  is determined from the slope,  $m$ , as  $q_e = 1/m$ . The adsorption rate constant ( $k_2$ ) is obtained from the intercept as  $k_2 = 1/(C \times q_e^2)$  and  $C$  is the intercept. The initial sorption rate,  $h$  ( $\text{mg g}^{-1} \text{min}^{-1}$ ) of metal ions describes the feasibility of the adsorption.

## 2.7. Adsorption isotherms

To investigate the quantitative Pb (II) ions adsorption, the adsorption isotherm models such as Langmuir, Freundlich and Temkin, were used.

### 1.1.1. Langmuir model

Langmuir model describes the adsorption at the specific homogenous active site [31]. The model assumes all active sites are similar to the small patches, which are energetically equal relative to each other, and the adsorption produces mono layer phenomenon. The Langmuir model is given in Eq. (7):

$$\frac{C_e}{q_e} = \left( \frac{1}{b} \right) (C_e) + \left( \frac{1}{b} \right) \left( \frac{1}{K_L} \right) \quad (7)$$

where  $C_e$  is the equilibrium concentration ( $\text{mg L}^{-1}$ ),  $q_e$  is the amount of metal adsorbed per unit adsorbent ( $\text{mg g}^{-1}$ ),  $K_L$  is the Langmuir equilibrium constant and  $b$  is the amount of metal ions required to form a mono layer ( $\text{mg L}^{-1}$ ). The plot  $C_e/q_e$  versus  $C_e$  gives the straight line with the slope  $m = 1/b$ , and the intercept  $C = (1/b) \times K_L$ . The feasibility of adsorption process could be calculated by using the separation factor,  $R_L$ , which is the dimensionless function of Langmuir model to determine the sorption ability of the sorbent materials :

$$R_L = \frac{1}{1 + bC_e} \quad (8)$$

### 1.1.2. Freundlich model

The Freundlich model describes the adsorbent surfaces with multi-functional groups having different energies. The active sites are heterogeneous in morphology. Linear form of adsorption model is given as follows [32]:

$$\ln q_e = \ln K_F + \frac{1}{n} \ln C_e \quad (9)$$

where  $K_F$  is the equilibrium constant, and  $n$  is the empirical constant. A plot of  $\ln q_e$  versus  $\ln C_e$  gives a straight line with the slope of  $1/n$ , and the Freundlich constant,  $K_F = e^C$ , and  $C$  is the intercept.

### 1.1.3. Temkin model

Temkin and Pyzhev [33] isotherm describes the interaction of adsorbate-adsorbate. Temkin model assumes thermodynamic feasibility of metal interaction on the adsorbent active sites and given as follows:

$$q_e = B \ln K_T + B \ln C_e \quad (10)$$

where the plot of  $q_e$  vs.  $\ln C_e$  gives a straight line, with slope  $B$  is related to the heat of adsorption, and  $K_T = e^{C/B}$  describes the equilibrium binding energy ( $\text{L mg}^{-1}$ ). The heat of adsorption of all the molecules in the layer decreases linearly with surface coverage due to the adsorbate-adsorbate interactions.

### 1.7. Desulphurization of diesel

Normal market diesel was purchased from the PETRONAS Petrol Station, Bandar Seri Iskandar, Perak, Malaysia. The total sulphur and carbon was determined using CHNS Analyser (Hitachi). One mL of sample was taken in Al-tube and placed in the furnace at high temperature under oxygen environment. Oxidized sample was burned into corresponding oxide such as  $\text{SO}_x$  and  $\text{CO}_x$  and the oxides formed were detected and recorded at the flame photometric detector (FPD). The 100 mL of diesel was placed in 250 mL Erlenmeyer flask and 1 g of sorbent was suspended. The flask was covered and placed on the orbital shaker at 150 rpm and room temperature ( $25 \pm 1^\circ\text{C}$ ) for 24 h. Lead-loaded cellulose sorbent was filtered out and the total sulphur and carbon content before and after the experiment were analyzed.

## 3. Results and discussion

### 3.1. Surface modification of PEC-OPEFB

Surface modification of PEC-OPEFB was carried out by directly reacting the hydroxyl ( $-\text{OH}$ ) group of anhydro-glucose with  $-\text{COOH}$  of acetic acid, oxalic acid and EDTA. The C-2, C-3 and C-6  $-\text{OH}$  groups of cellulose unit molecule are readily available as reactive sites for esterification. Each anhydro-glucose unit can be modified by three  $-\text{COOH}$  of acetate (1), oxalate (2) and EDTA (4) groups and the  $-\text{COOH}$  substituted groups can be identified by determining the degree of substitution (DS) as given in Table 1. Raw cellulose does not contain any carboxylic functionality, as structurally it contains 3  $-\text{OH}$  groups which can be modified with carboxylic acids. The DS describes the reagents penetration into the non-crystalline portion and suggests the potential amount of carboxylic group present on the cellulose. The oxidation of anomeric carbon at C1 in the order of  $0.3\text{--}0.6 \text{ mmol g}^{-1}$  may be possible for singular glucose unit. However, the H-bonding of crystalline region could limit further substitution as the DS also depends on the structure of reactive groups where the bulky structure of attacking groups may reduce the substitution due to the steric hindrance.

The maximum number of carboxylic group substitution can be up to 3 due to the availability of 3-OH groups of MAcUS and MAcAUTO. The DS were 1.95 and 1.67, respectively, which was agreeable to the reported value of 1.94 for cellulose [34]. The substitution of dicarboxylic groups (oxalic acid) of MOUS and MOAUTO were however lower at 1.29 and 1.18, respectively. EDTA with its bulky nature, which restricts the attack and limits the substitution of MEUS and MEAUTO to 0.778 and 0.874, respectively. The lower DS suggests the lesser substitution of cellulose due to structural limitations. The acetate, oxalate, and EDTA

possess one, two and six donor atoms with electron pairs (ligands), respectively. Having more than two electron pair donor atoms present in the group is designated as a polydentate. The metal loading onto the sorbent is directly proportional to the number of ligand present on the sorbent. Therefore, despite the lower DS of MEUS and MEAUTO, they may actually possess higher metal chelating ability due to the presence of polydentate ligand.

### 3.2. Morphological characterization

Raw OPEFB has a compact structure, tightly packed with hemi cellulose, cellulose and lignin with deposition of waxes (Fig. 1a). The external surface of PEC-OPEFB showed a mixture of smooth surface with scars, highly likely due to the removal of inorganic particles such as the metal components, and the sputtering of silica (Fig. 1b) [25, 26]. Figs. 1c–h show the surface of cellulosic fiber becoming rough with cracks and holes which confer good properties for effective sorbent material. The layered structure of the PEC-OPEFBs with the visible pores and uneven surface upon modification were potentially due to the reagent substitution on the surface such as the grafting of acetate group (Figs. 1c,d). With oxalate, and similarly observed with EDTA-grafting, the surface texture showed non-smooth layered structure with more visible spacing, cracks and holes (Figs. 1e,f). The uneven surfaces suggest the non-uniform grafting of the carboxylic groups (mono, di and polydentate ligands) and the different amount of active sites distribution as suggested by the differences in DS (Table 1).

### 3.3. Chemical characterization

Raw OPEFB showed peaks associated with hemicelluloses and lignin (carbonyl functionality) at  $1248 \text{ cm}^{-1}$  and  $1735 \text{ cm}^{-1}$  [25,26] which were absent from the extracted PEC (Figs. 2a,b). The peaks at  $1635 \text{ cm}^{-1}$  and  $1648 \text{ cm}^{-1}$  are the characteristic peaks of water O-H stretching. The peak at  $2902 \text{ cm}^{-1}$  is attributed to the C-H stretching of  $\text{CH}_2$  and  $\text{CH}_3$ . The peaks at  $1047$  and  $980 \text{ cm}^{-1}$  representing the  $\beta$ -glucosidic linkage in the cellulose chain [26,35,36] are present in all spectra. The differences in the peak shapes at  $3364 \text{ cm}^{-1}$  and  $1734 \text{ cm}^{-1}$  of acetate, oxalate and EDTA-modified sorbents proved that the  $-\text{COOH}$  groups were replacing and substituting the H from  $-\text{OH}$  groups of cellulosic an hydro-glucose unit, suggesting successful structural changes (Figs. 2c–h) and surface modification. The relative low or high peak intensities can be correlated to the amount of  $-\text{COOH}$  grafting with the degree of substitutions. The surface modification gives understanding on the singular effect of known amount of mono, di and poly carboxylic groups towards metal ion sorption.

### 3.4. Heavy metal ion adsorption

#### 3.4.1. Effects of pH

pH is an important factor that affects the adsorption of metal ions onto the sorbent surface and the degree of ionization of different metal ions in the solution. At specific pH, changes in the sorbent structures and active sites could affect

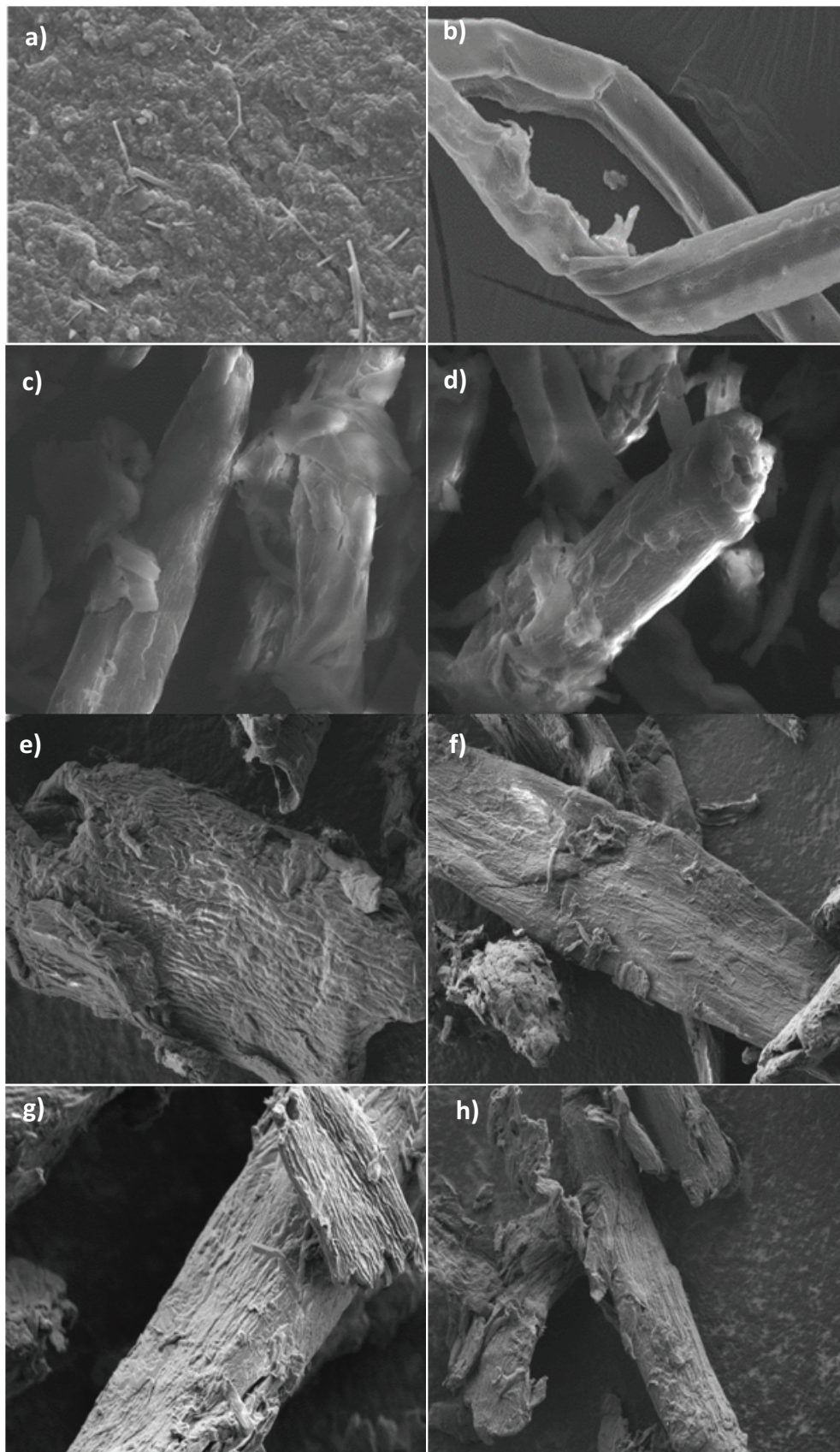


Fig. 1. FESEM images of (a) Raw OPEFB, (b) PECs, (c) MACUS, (d) MACAUTO, (e) MOUS, (f) MOAUTO, (g) MEUS and (h) MEAUTO.

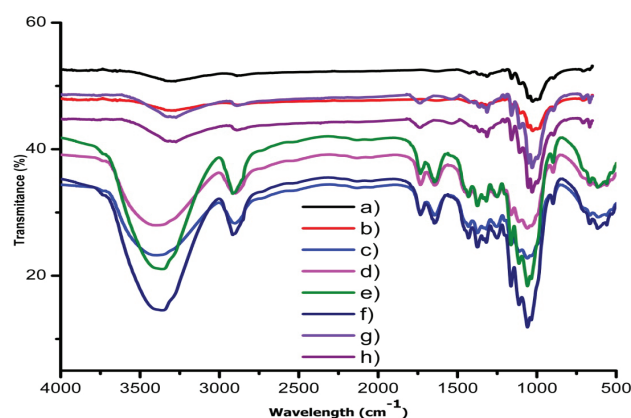


Fig. 2. FTIR spectra of a) PEC-US; b) PEC-AUTO; c) MAcUS; d) MAcAUTO; e) MOUS; f) MOAUTO; g) MEUS; and h) MEAUTO.

the metal uptake. The effect of pH changes from 4–8 on Pb (II) ion sorption on the M-PECs are shown in Fig. 3. At low pH, the carboxylic groups ( $-\text{COOH}$ ) formed carboxyls on the sorbent surface through accepting the lone pair from the oxygen atom of  $-\text{COOH}$ . The low Pb (II) ion uptake at pH 4 could be due to the high concentration of  $\text{H}^+$  and  $\text{H}_3\text{O}^+$  ions competing with positive cations for the adsorption sites [4]. The small size of  $\text{H}^+$  also results in faster rate of attachment to the active sites than do the divalent metal ions.

With increase in pH, the carboxyls turn into carboxylate anions and the acidic groups of  $-\text{COOH}$  may also dissociate, leading to more interaction between positively charged metal ions and the negatively charged carboxylate ions or the hydroxide ( $-\text{OH}$ ) groups on the sorbent surface through hydrogen bonding or ion exchange mechanisms. The Pb (II) uptake ( $\text{mg g}^{-1}$ ) was optimum at pH 6 for MAcUS (70.5), MOUS (77.1), MEUS (88.5) and MAcAUTO (69.8), MOAUTO (72.2), MEAUTO (86.5) (Figs. 3a & b). In comparison, the Pb (II) sorption capacity ( $\text{mg g}^{-1}$ ) at pH 6 are as follows: *P.chrysosporium* (85.9), sugarcane bagasse (133.6), cellulose-imidazole (75.8); and at pH 5.5: the grape stalk (49.9) and sugar beet pulp (73.8) [23]. At more basic pH, there will be less competition between  $\text{H}^+$  and the metal ions for active sites due to reduced  $\text{H}^+$ . Lone pairs of sorbent active sites are more readily available to bind with the metal ions. The lower the number of lone pairs from the active sites, the lower shall be the metal chelation. However, when the pH is above the optimum, the metal uptake started to equilibrate and dropped at pH 8. The increased hydroxide ions ( $\text{OH}^-$ ) may cause the positively charged metal ions to form stable hydroxides. The tendency is for the metal ions to detach from the binding sites, forming stable white  $\text{Pb}(\text{OH})_2$  precipitates in the working solution.

#### 3.4.2. Effects of contact time at different initial concentration

The adsorption behaviour of M-PECs was investigated at different initial concentration of 100–500 ppm, for contact time of 0–360 min at pH 6 and 150 rpm agitation (Fig. 4). The equilibrium time achieved for initial concentration of 100, 200, 300, 400 and 500 ppm was 60, 120, 180, 240 and 240 min, respectively. This is attributable to the large availability of Pb

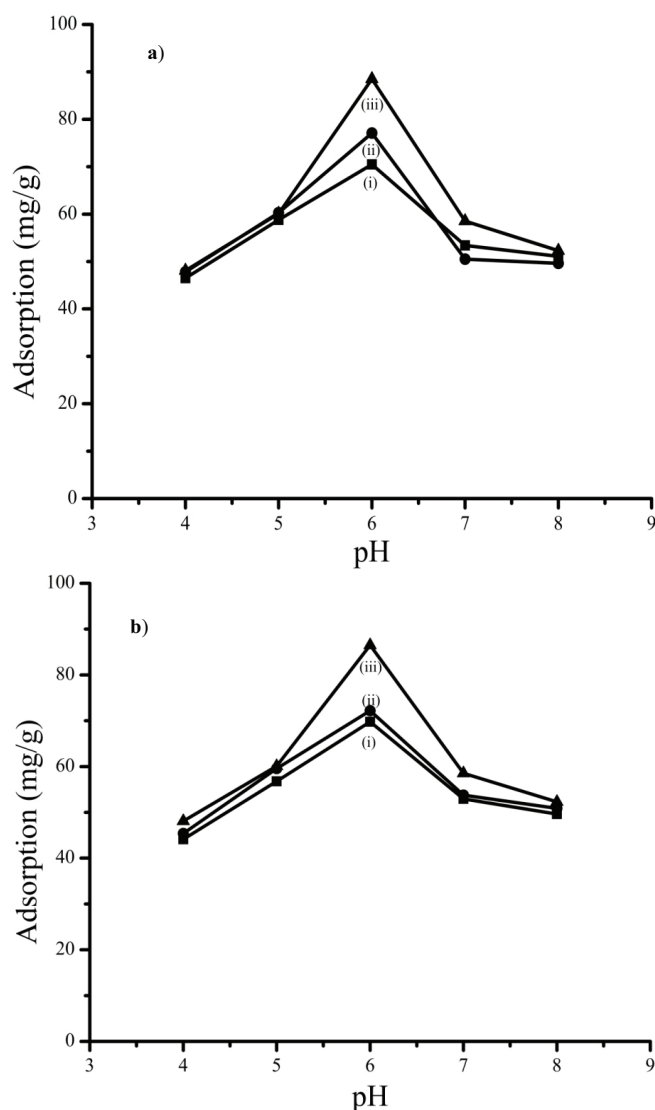


Fig. 3. Effects of pH on Pb (II) sorption by M-PECs from (a) SONO-CHEM: (i) MAcUS, (ii) MOUS, (iii) MEUS; and (b) AUTO-CHEM: (i) MAcAUTO, (ii) MOAUTO, (iii) MEAUTO.

(II) ions with increased concentration, resulting in the corresponding longer equilibrium time. The sorption rate was initially high due to the availability of maximum active sites [37], but becoming slower towards reaching the equilibrium due to the lesser active sites remaining. Maximum removal of Pb (II) ions were achieved at all tested concentrations and all active sites could have been occupied completely after 240 min. Lead ion possesses the ionic size of 133 pm which may affect the ion occupancy rate on the active sites [1]. However, the large number of metal ions should enhance the probability of attachment to the active sites.

The higher the DS, the more number of  $-\text{COOH}$  groups attached to the cellulose  $-\text{OH}$ , and this should result in higher metal uptake. However, the trends were in the order of: MEUS/MEAUTO > MOUS/MOAUTO > MAcUS/MAcAUTO. The polydentate (EDTA) exhibited stronger chelating behaviour than the bidentate (oxalate)

and monodentate (acetate). The sorption capacity of Pb (II) ( $\text{mg g}^{-1}$ ) with MEAUTO (236.7) (Fig. 4f) was comparable to MEUS (232.9) (Fig. 4c). Despite the lower DS, the MEUS/MEAUTO sorbents possess four carboxylic groups and two amino groups (Table 1) allowing for maximum chelation. As shown in Table 2, our sorbents achieved higher sorption capacity than the Modified-Soda Lignin (MSL)-EFB (46.7), sugar bagasse (133.6), the modified celluloses and woods

(6–105) [23], the agro-wastes (27–125) [38,39] and marine algae (33.5) [40]. Only the EDTA-modified sugar bagasse achieves the highest sorption at  $333 \text{ mg g}^{-1}$  [41].

### 3.4.3. Pseudo-first order and second order kinetics

Pseudo-first order and Pseudo-second order kinetic models for Pb (II) ions sorption at 300 ppm were investi-

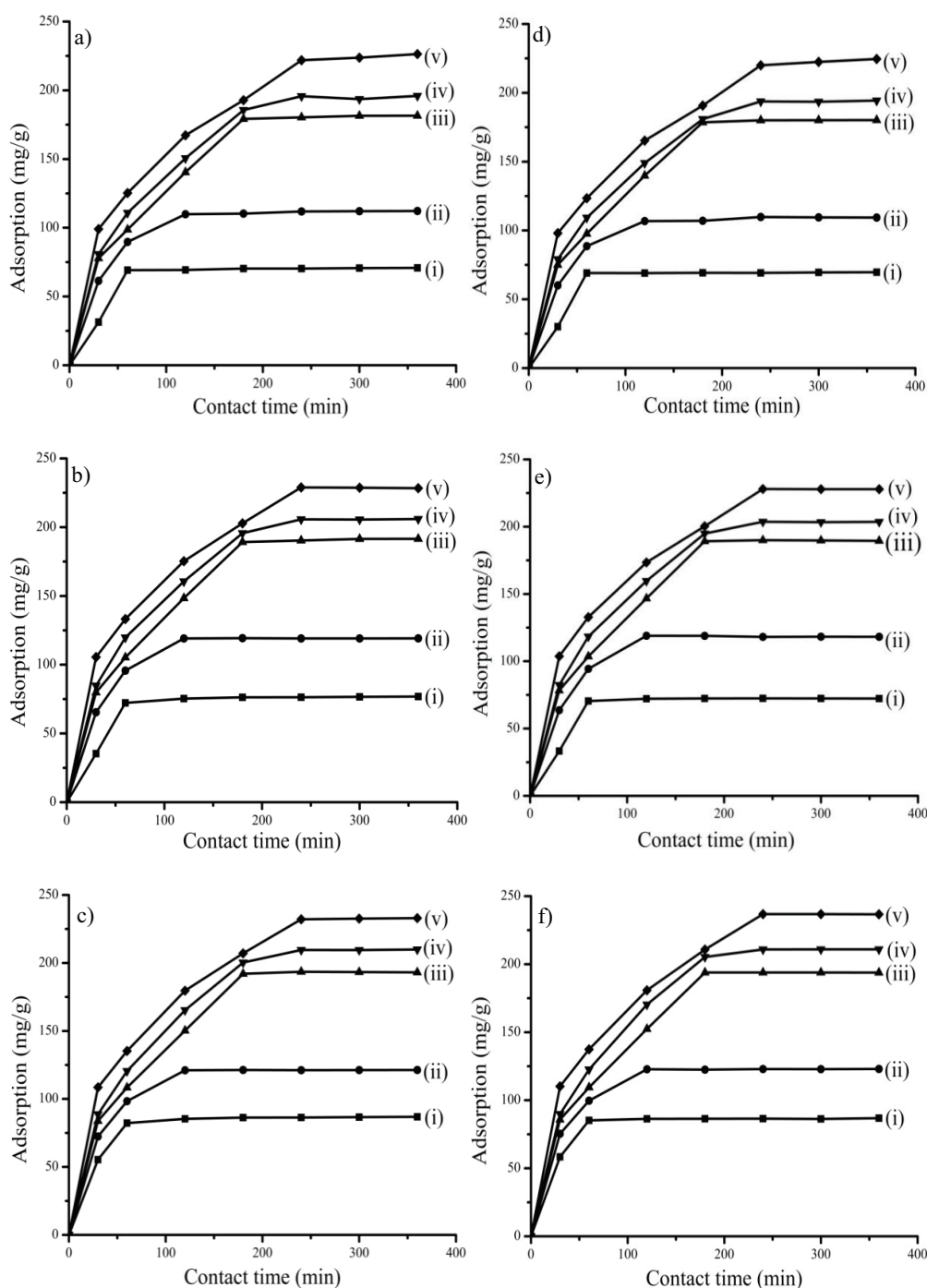


Fig. 4. Effects of contact time on Pb (II) sorption by M-PECs from (a–c) SONO-CHEM, (d–f) AUTO-CHEM, at initial concentrations of (i) 100 ppm, (ii) 200 ppm, (iii) 300 ppm, (iv) 400 ppm, (v) 500 ppm.



Table 2  
Sorbents and the metal adsorption capacities

Sorbent	Pb <sup>2+</sup> (mg/g)	Reference
Sugar bagasse	133.6	[23]
Cellulose-acrylic acid	55.9	
Cellulose-imidazole	75.8	
Wood-acrylate	6.0	
Wood-citric acid	83.0	
Cellulose-butanedioic acid	105.0	
Cellulose- $\alpha$ -thioglycerol	6.0	
Cellulose-3-mercaptopropionic acid	20.0	
Cellulose-2-aminoethanethiol	81.0	
Grapes stalk waste	49.9	
<i>P. chrysosporium</i>	85.9	
Clinoptilolite	124.0	
Oil palm fiber	125.0	[38]
Activated-OPEFB-carbon	48.96	
Rice husk-tartaric acid	120.8	
Pinus-wood-citric acid	82.64	
Palm shoot-mercaptopropionic acid	52.86	
Corn-Sulphuric acid	124.0	
Wheat-bran-sulphuric acid	55.56	
Dates stem-nitric acid	27.03	
MSL-EFB	46.72	[39]
<i>Durvillaea potatorum</i>	33.5	[40]
Sugar bagasse-EDTA	333.0	[41]
MAcUS	226.4	Our study
MAcAUTO	224.6	
MOUS	228.4	
MOAUTO	227.9	
MEUS	233.0	
MEAUTO	236.7	

gated to ascertain whether the rate of Pb (II) ions sorption is independent or dependent on the initial concentration of metal ions, respectively. The kinetics parameters (Table 3) suggest that the pseudo-second order kinetics can best describe the sorption of all sorbents based on  $R^2 > 0.97$ – $0.98$  (Fig. 5). The rate of reaction clearly depends on the initial concentration of Pb (II) and there is an interaction of Pb (II) with sorbent at equilibrium. The rate constants were calculated as  $4.86$ – $6.41 \text{ g}^{-1} \text{ mg}^{-1} \text{ min}^{-1}$  and the initial rate of reactions were  $199$ – $212 \text{ mg g}^{-1} \text{ min}^{-1}$ . Other studies have also reported the pseudo-second order kinetics as the best model to describe the Pb (II) sorption onto Poly(hydroxamic acid) (PHA)-grafted-EFB and the fern biomass sorbents, suggesting the chemisorptions between the metals ions and the sorbent [38,42]. In the case of PHA-grafted-EFB, the chemisorption of Pb(II) is proposed via hydroxamic acid [38], while the M-PECs sorbents in our study could have interacted via the carboxylic groups.

#### 3.4.4. Adsorption isotherms

Adsorption isotherms are important theoretical models to describe the adsorption characteristics of any sorbent material. Langmuir isotherm elucidates the mono layer formation on the sorbent by the sorbates and applicable only when all the active sites are homogeneously equivalent. Langmuir equation [Eqs. (7), (8)] is used for the plot of  $C_e/q_e$  versus  $C_e$  (data not shown), and the parameters are presented in Table 3. The  $R^2$  values are in the range of  $0.958$ – $0.965$  suggesting that the sorption may follow Langmuir adsorption. The Langmuir constant,  $b$ , at  $0.55$ – $0.801$ , which is greater than zero, and the separation factor,  $R_L$ , within  $0$ – $1$  range, may suggest the feasibility of mono layer adsorption process onto the M-PECs sorbents. The constant,  $b < 1$  and  $R_L < 1$  also suggest the model fitness. However, the  $R_L = 0.0069$ – $0.01$  ( $R_L \approx 0$ ) instead suggests unfavourable condition for metal attachment to the active sites, and therefore unfavourable for Langmuir adsorption. Similar observation has been made for *Cladophora rivularis* with  $R_L = 0.0639$  for Pb (II) sorption [43]. Langmuir isotherm for Pb (II) sorption has been reported on materials such as wood-citrate (3-carboxylic acid), OPEFB-activated carbon, OPEFB-hydroxamate (R-C(O)NH-OH), palm-mercaptopropionate ( $\text{C}_2\text{H}_4\text{O}_2\text{S}$ ) and rice husk-tartaric acid ( $\text{HO}_2\text{CCH}(\text{OH})\text{CH}(\text{OH})\text{CO}_2\text{H}$ ) [38], cellulose-monocarboxylic acid, cellulose-imiazole, and *Phanerochaete chrysosporium*, *Trametes versicolor*, sugar-beet-pulp and lignin-bagasse [23]. The carboxylic, nitrogen and sulphur atoms can act as ligands to hold Pb (II) metal ions to form mono layers. The suitability of Langmuir isotherm model using cetyltrimethyl ammonium bromide (CTAB) surfactant-modified carbon for Cd (II) sorption has been attributed to the increase in the mono layer capacities of the adsorbents after treatment with surfactants. This is suggested to indicate the superior homogeneity of the available surface area potentially due to the formation of a uniform micro crystalline layer of the surfactant molecules on to the adsorbent surface, which in turn enhance the available surface areas, porosity and pore volumes [4].

Freundlich adsorption model suggests sorption as the heterogeneous multilayer phenomenon. Based on the linear coefficient  $R^2$  of  $0.9699$ – $0.9754$  (Table 3), our M-PECs sorbent parameters are better fitted to Freundlich than Langmuir isotherm. The  $K_F$  and  $1/n$  values which determine the feasibility of adsorption process of Pb (II) ions for  $2 < K_F < 10$  and  $1/n < 1$  showed the  $K_F$  of  $2.42$ – $2.58$ ; and  $1/n$  of  $0.76$ – $0.91$ , suggesting that the adsorption is feasible with the formation of heterogeneity on the sorbent surfaces. These are far higher than the value of  $1/n = 0.4710$  for Pb (II) on *Cladophorarivularis* sorbents [43] which confirms the efficiency of four sorbents. The availability of grafted carboxylic groups and pores contribute towards heterogeneous active sites for the attachment of Pb(II) ions. The modified lignocellulosic sorbents such as *Trametesversicolor*, orange peel, cellulose-pulp-acrylate, sunflower stalks-amidoxime [23] have all reported the Freundlich isotherms as the best to describe the divalent metal ions sorption.

Temkin isotherm describes the formation of interaction between metal ions and sorbents. Temkin equation (Eq. (10)) is used for the plot of  $q_e$  vs.  $\ln C_e$  (Fig. 6), and the parameters are presented in Table 3. The  $R^2$  of  $0.978$ – $0.983$  suggest that Temkin adsorption isotherm is the best to describe the adsorption of Pb(II) on M-PECs. The equilibrium bind-

Table 3  
Kinetics and adsorption isotherm parameters for Pb(II) sorption on M-PECs

Parameters / Sorbents	MAcUS	MOUS	MEUS	MAcAUTO	MOAUTO	MEAUTO
Pseudo-First order	9.756	10.012	10.098	12.696	9.662	9.563
$q_e$ (mg/g)						
$k_1$ (min <sup>-1</sup> )	0.020	0.018	0.207	0.295	0.020	0.025
$r^2$	0.832	0.834	0.914	0.9549	0.8767	0.7593
Pseudo-Second order	5.72	5.99	6.38	5.59	5.89	6.62
$q_e$ (mg/g)						
$k_2$ (g mg <sup>-1</sup> min <sup>-1</sup> )	6.12	5.92	5.22	6.41	6.12	4.86
$h$ (mg g <sup>-1</sup> min <sup>-1</sup> )	199.9	212.8	212.8	200.0	212.8	212.8
$r^2$	0.9785	0.9786	0.98	0.9774	0.9771	0.9809
Langmuir	0.583	0.697	0.769	0.550	0.670	0.801
$b$ (mg/g)						
$K_L$ (L/mg)	87.959	80.189	76.923	89.990	81.492	75.618
$R_L$	0.0094	0.00791	0.00716	0.0100	0.0082	0.0069
$r^2$	0.9645	0.9590	0.9630	0.9610	0.9580	0.9650
Freundlich	2.42	2.51	2.56	2.395	2.484	2.578
$K_F$ (mg/g)(L/mg) <sup>1/n</sup>						
$N$	1.286	1.175	1.1207	1.323	1.197	1.099
$1/n$	0.777	0.850	0.890	0.755	0.835	0.909
$r^2$	0.9754	0.9701	0.9716	0.9736	0.9699	0.973
Temkin						
$K_T$ (L/mg)	324.660	329.813	331.663	324.041	329.241	331.931
$B$	-183.96	-176.2	-174.29	-184.73	-176.96	-173.68
$r^2$	0.9827	0.9798	0.9783	0.9834	0.9804	0.9779

ing constants at 324–331.9 L mg<sup>-1</sup> for all M-PECs sorbents suggest high binding strength of bivalent metal ions onto the surfaces with the sorbents heat of sorption of -173.68 to -183.96 J mol<sup>-1</sup>. The oxygen containing ligands binding energy with metal ions are in the range of 0–30 kJ mol<sup>-1</sup> [44]. The equilibrium-binding constants vary when sorbent structures are changed from monodentate to polydentate ligand. As the DS of sorbents suggest the number of binding sites available on the sorbent, the O-atom can act as ligand for the uptake of metal ions through complex formation. When 1 mole of Pb(II) ions bind with 1 mole of sorbent active sites at equilibrium, heat is released suggesting that the binding is exothermic in nature and could take place at room temperature [44].

### 3.4.5. Mechanism of Pb(II) ion adsorption

Based on the kinetics and isotherms model established, the Pb(II) ion sorption on the M-PECs sorbent is clearly dependant on the initial Pb(II) ion concentration, forming heterogeneous multilayer adsorption on the sorbent surface with heat released due to high binding strength. Different steps may be involved in the adsorption process including ion sorption on the pore surface, pore diffusion, film or external diffusion and surface diffusion. Intra-particle diffusion involves the diffusion of metal ion from the bulk of the external surface into the sorbent pores [45]. The rate may

be controlled by the ion concentration, the ionic size of the molecule, the affinity between the ions and the sorbent, the pore-size distribution, the diffusion coefficient of the ions, and the mixing efficiency [46]. The intraparticle diffusion model (data not shown) based on Pb(II) ion sorption on the raw OPEFB and PECs suggests the three stages involved:- the fast rate of external surface sorption; the gradual sorption stage where intra-particle diffusion is the rate-limiting step; and the declining intra-particle diffusion rate due to the reduction of ion concentration in the bulk solution [47]. Other mechanisms that have been proposed to describe the adsorption behaviours on sorbents include the electron donor-acceptor complex, the  $\pi$ - $\pi$  dispersion interactions, the solvent effects [48] and factors such as dispersive force, induction force and ion-exchange interactions [49].

Comparing the structure in Table 1 with the proposed ion interactions with the sorbent in Fig. 7 elucidates the importance of O- and N- atoms of elements from periodic table group V and VI. The electronic configuration member of O and N-atom provide the electrons lone pairs (non-bonding) to form chelate-interaction with metal cations. Although the carboxylic groups (-COOH) show weak interactions with Pb(II) ions through the lone pair of oxygen atoms [23], sorbents grafted with different amount of mono carboxylic (acetate), dicarboxylic (oxalate) and poly carboxylic acid (EDTA) functional groups exhibit different extent of Pb(II) uptake. While the DS describes the number of groups that can be substituted on the an hydro glucose

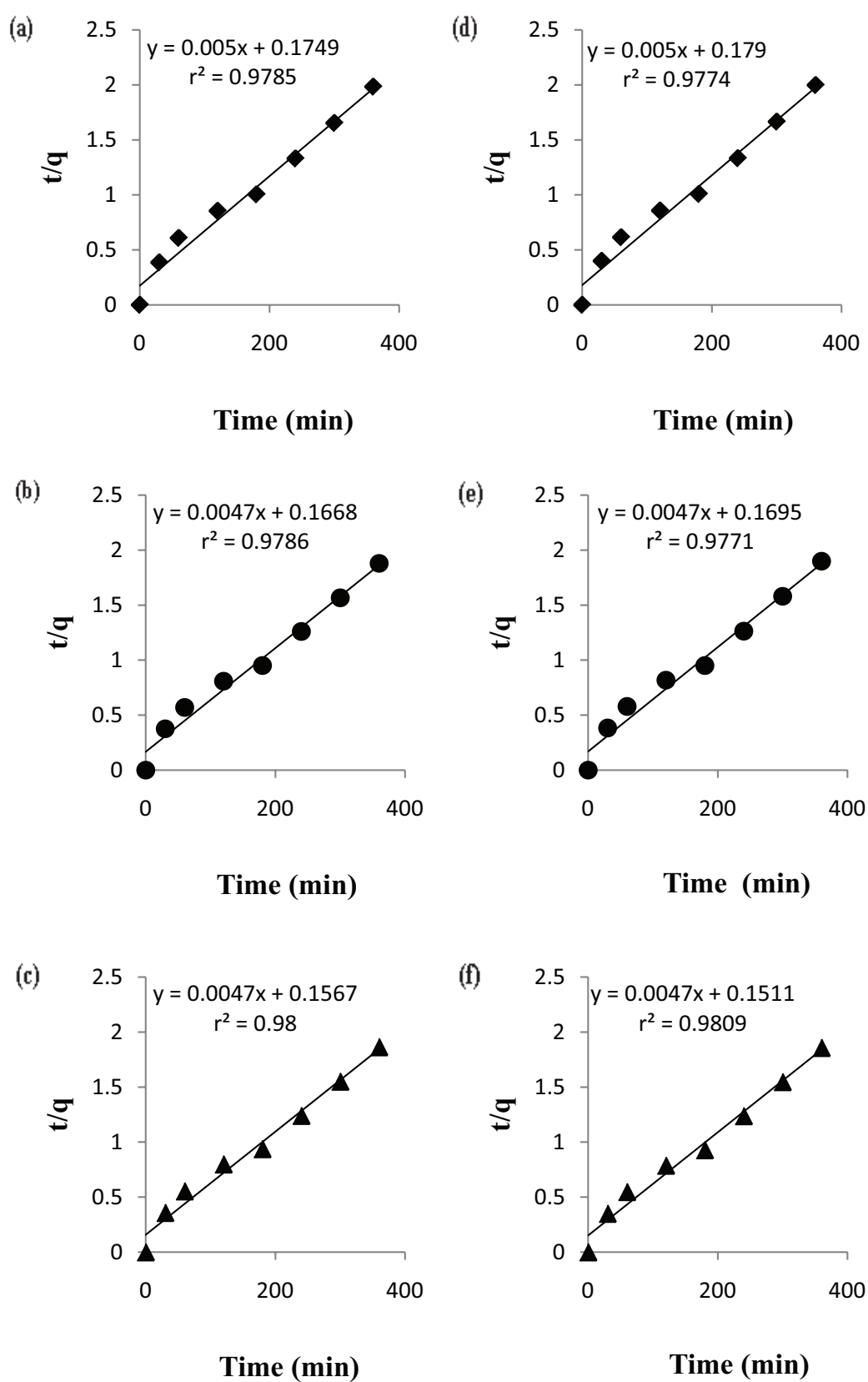


Fig. 5. Pseudo-second order kinetics for Pb(II) sorption at 300 ppm on (a) MACu, (b) MOUS, (c) MEUS, (d) MACAUTO, (e) MOAUTO and (f) MEAUTO, at pH 6 and 150 rpm agitation speed.

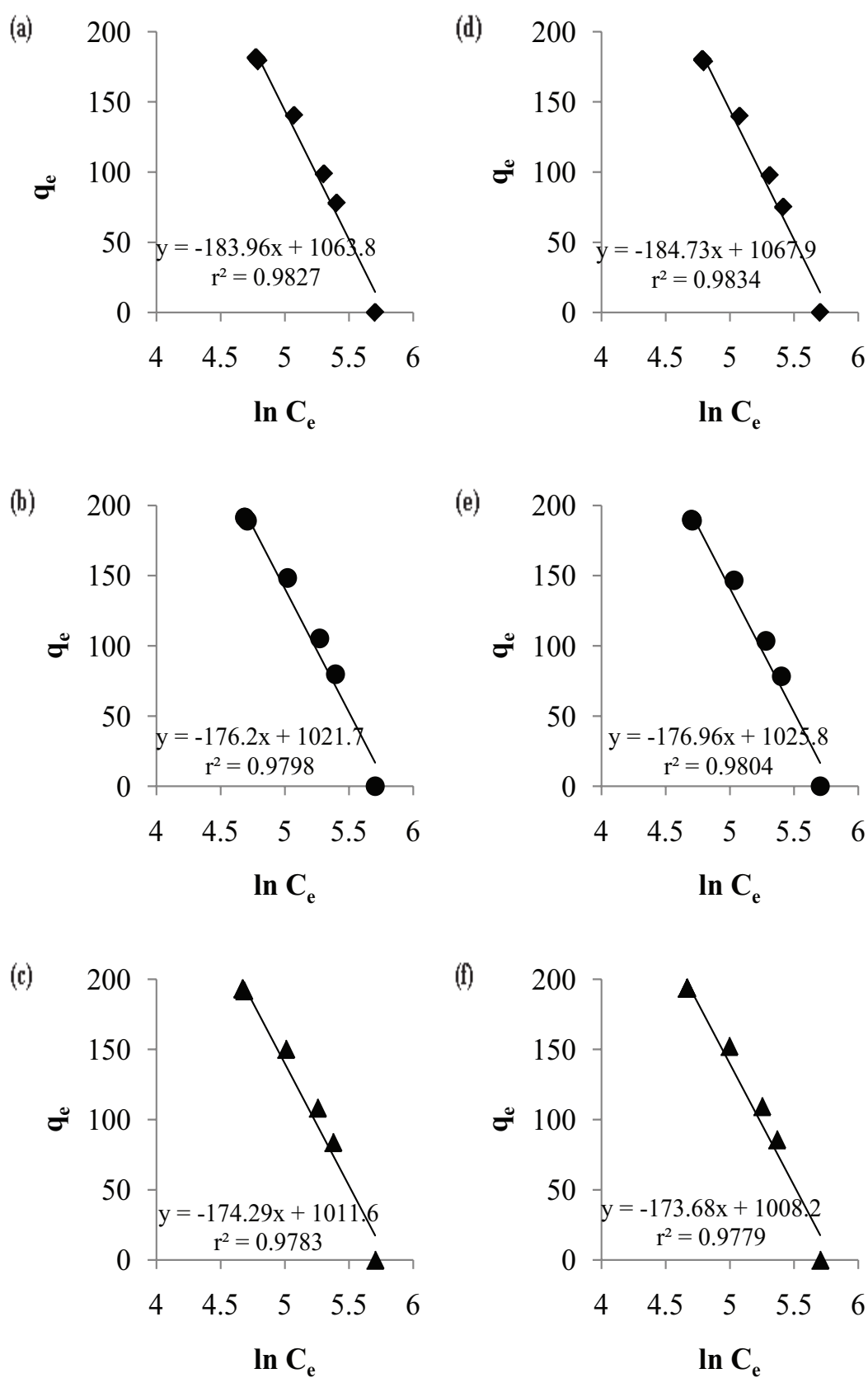


Fig. 6. Temkin isotherm for Pb(II) sorption at 300 ppm on (a) MACu, (b) MOUS, (c) MEUS, (d) MAcAUTO, (e) MOAUTO and (f) MEAUTO, at pH 6 and 150 rpm agitation speed.

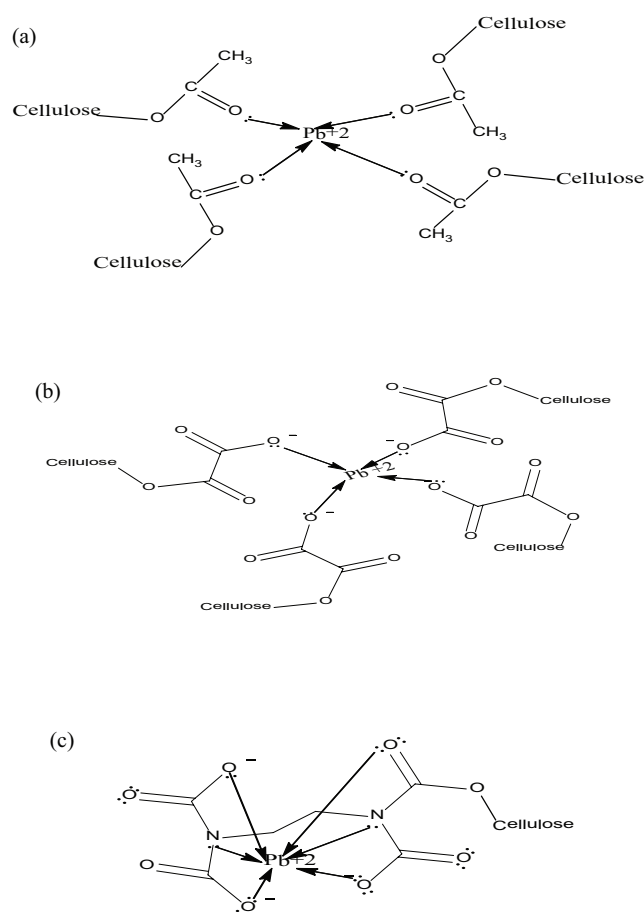


Fig. 7. Potential chemical interactions of Pb (II) with (a) Acetate; (b) Oxalate; (c) EDTA.

unit of the cellulose chain, both the number of functional groups and the number of ligands on the functional groups are actually equally important.

The greater the number of grafting groups, the higher the chances for the metal ions being loaded onto the sorbents. The metal ions ( $M^{2+}$ ) d-orbital generates interaction by accepting the electron pair from the ligand containing  $-COOH$  group [23]. Cellulose derivatization can be carried out by oxidation of cellulose. Cellulose dialdehyde for example is obtained by reacting the cellulose with periodate before further oxidation by chlorite. The solubility also depends on the oxidation where 70% oxidized cellulose may yield large insoluble fraction, while 100% oxidized cellulose may be completely soluble in water. Metal adsorption capacity of dialdehyde cellulose has been increased from  $184 \text{ mg g}^{-1}$  to  $246 \text{ mg g}^{-1}$  based on the synthesized cellulose-hydroxamic acid [50]. Esterification of wood cellulose in which the ester bond ( $R-CO-O-R$ ) is formed can be achieved by reacting the carboxylic anhydride with cellulose. acetic, oxalic and citric acid are heated to remove water molecules from the anhydride. The H-atom of cellulosic  $-OH$  group will be substituted by the carboxylic group and the carboxylic acid substitution increases the fiber affinity towards divalent metallic ions such as Cu and Pb [51].

The  $-COOH$  groups present on the cellulose chains may involve in the interaction where the O-atom of acetate groups of MAcUS and MAc AUTO donate the electron pair to Pb (II) which hold the metal ions together (Fig. 7). Despite the bulkier oxalated-cellulose and having the DS lesser than the acetated-cellulose, the oxalate-M-PEC produces better interaction and higher metal ion sorption which are attributable to the two  $-COOH$  groups available for metal chelation. The EDTA-M-PEC has the lowest DS because of its least reactivity and bulkier structure, yielding high steric hindrance for substitution on the anhydro glucose unit of PEC. Yet, the high metal sorption capacity achieved with EDTA is due to the four O-atoms and two N-atoms with electron pairs acting as ligands, confirming the importance of having six lone pair donor (ligand) groups on each EDTA to chelate the Pb (II) ions.

### 3.5. Desulphurization of diesel

The initial total sulphur content in diesel that constitutes thiophene, benzothiophene, and dibenzothiophene was 670 ppm (Table 4). The MAcUS, MOUS and MEUS reduced the S content by 50, 110 and 80 ppm, respectively, as compared to the Pb (II)-loaded oxalate and EDTA which reduced the S by 300 (44.7%) and 350 (52.2%) ppm. The total carbon content in diesel before treatment was 84.1 ppm and the C content was reduced by 1.08, 0.86 and 0.34%, respectively, as compared to the Pb (II) loaded MAcUS, MOUS and MEUS which had reduced the C-content by 3.94, 4.17, and 4.27%, respectively. The Pb (II)-loaded sorbents therefore enhanced the C and S removal by almost 4–12 folds for C and 3–5 fold for S.

To illustrate the phenomenon of sulphur sorption onto the Pb (II)-loaded M-PECs sorbent, the basic structure of thiophene is used as a theoretical model. The thiophene resonance structures are shown in Fig. 8. Having S-atom with positive charge (during resonance) could lead to the attraction to the O-atom of  $-COOH$  group, while the negatively charged C-atom of S-compounds may interact with the positively charged Pb (II) ions on the sorbent. The  $-COOH$  functionalities are responsible for the interaction between the positively charged S-compounds with the negatively charged ( $-COO$ ) or the electron pair of O-atom ( $-COOH$ ). With ionic radius of Pb (II) at 133 pm, there may be greater outer surface available for the interaction with the negatively charged C-atom of S-compounds. The reduction of total sulphur content may include the removal of small ring (thiophenes) and complex ring structured (polyaromatic thiophenes, benzothiophene, and dibenzothiophene) of S compounds. The reduction in carbon content in diesel was minimal around 1–4% due to the removal of organic sulphur present in the carbon skeleton (Fig. 8).

The high S removal and low C content reduction suggest the efficacy of the M-PECs sorbents to play dual functions in environmental remediation - firstly for the M-PECs as heavy metals removal from the wastewater, and secondly for the metal-loaded M-PECs utilization in the desulphurization of diesel. In the sorbent material development, metal selection is important to ensure strong interaction with the surface species of the matrix with the size of about 10 nm. The metal should be the type that provides high electron attraction to interact with sulphur compounds present in the hydrocarbon feed. The metal should ideally be from a

Table 4  
Sulphur and Carbon content in diesel before and after sorbent treatment

Modified sorbent	Diesel before treatment		Diesel after treatment		Total reduction	
	S (ppm)	C (%)	S (ppm)	C (%)	S (ppm/%)	C (%)
	670	84.1	–	–		
MAcUS	–	–	620	83.0	50/7.5	1.08
MOUS	–	–	560	83.2	110/16.4	0.86
MEUS	–	–	590	83.8	80/11.9	0.34
Pb-MAcUS	–	–	390	80.2	280/41.7	3.94
Pb-MOUS	–	–	370	79.9	300/44.8	4.17
Pb-MEUS	–	–	320	79.8	350/52.2	4.27

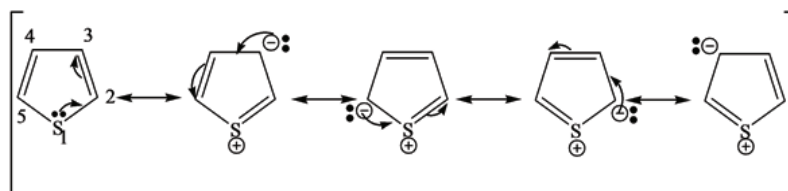


Fig. 8. Resonance structures of Thiophene.

$d^5$ – $d^{10}$  electron configuration, holding suitable oxidation states, and this include most of the transition metal elements from the first to third row of the Periodic Table of elements [52], and especially from the group IB, IIB, VIIB, and VIII for desulphurization. Metal impregnation including  $Pd^{2+}$ ,  $Fe^{3+}$  or  $Cu^{2+}$  have been applied on the porous organic polymer of poly-methylbenzene for desulphurization via adsorption technique [53]. To enable metal ion dispersion on the surface, the acceptable surface area range is estimated between  $400$ – $1200$   $m^2 g^{-1}$ . The higher the surface area of the matrix, the better will be the sorption of organosulphur compounds [54]. It is also important to render the adsorption to be reversible so that the used metal could be regenerated or the sorbents can be reused as in the case of magnetic biosorbents based on OPEFB, cellulose and *Ceiba pentandra* fibers [7,47]. The agro-based lignocellulosic materials fit the criteria for the mass production of cost-effective sorbent material for the applications in environmental remediation, waste water treatment and fuels and flue gases clean-up in the integrated biorefinery set-up [55–58].

#### 4. Conclusion

Surface modified PECs from OPEFB had been successfully developed as biosorbent with high sorption capacities for Pb(II) removal and desulphurization of diesel. Modifications of PECs were made with acetate (mono carboxylic), oxalate (di carboxylic) and EDTA (tetracarboxylic group). FESEM analyses showed rough structure with pores, cracks and holes, important as active sites for metal ion sorption, alongside the  $-COOH$  functional group in the carboxylic grafting as confirmed by the FTIR spectral data. The sorption capacities of sorbents for Pb (II) ions showed MEUS and MEAUTO achieving the highest sorption at  $232.9$   $mg g^{-1}$

and  $236.7$   $mg g^{-1}$ , respectively. Pseudo second order kinetics model best described the sorption process with rate constants of  $4.86$ – $6.41$   $mg g^{-1} min^{-1}$  and the initial rate of reaction of  $199$ – $212$   $mg g^{-1} min^{-1}$  and the adsorption was best fitted to the Temkin isotherms. The desulphurization of diesel using Pb-loaded MOUS and MEUS gave  $44.8$  and  $52.2\%$  sulphur removal, respectively. The biosorbent developed should be ideal for economical environmental remediation, waste water treatment, and fuels and flue-gases clean-up.

#### Acknowledgments

This work was partly supported by Biomedical Technology Mission-oriented Research (MOR), under Bioengineering Research group, Universiti Teknologi PETRONAS. Scholarship to Muhammad Shahid Nazir is acknowledged.

#### References

- [1] B. Alizadeh, M. Ghorbani, M.A. Salehi, Application of polyrhodanine modified multi-walled carbon nanotubes for high efficiency removal of Pb (II) from aqueous solution, *J. Mol. Liq.*, 220 (2016) 142–149.
- [2] E. Üçüncü Tunca, K. Terzioğlu, H. Türe, The effects of alginate micro spheres on phytoremediation and growth of *Lemna minor* in the presence of Cd, *J. Chem. Ecol.*, 33 (2017) 652–668.
- [3] M.O. Abd El-Magied, A.A. Tolba, H.S. El-Gendy, S.A. Zaki, A.A. Atia, Studies on the recovery of Th (IV) ions from nitric acid solutions using amino-magnetic glycidyl methacrylate resins and application to granite leach liquors, *Hydro metallurgy*, 169 (2017) 89–98.
- [4] M. Nadeem, M. Shabbir, M.A. Abdullah, S.S. Shah, G. McKay, Sorption of cadmium from aqueous solution by surfactant-modified carbon adsorbents, *Chem. Eng. J.*, 148 (2009) 365–370.

- [5] A. Zahid, A. Shah, F.J. Iftikhar, A.H. Shah, R. Qureshi, Surfactant modified glassy carbon electrode as an efficient sensing platform for the detection of Cd (II) and Hg (II), *Electrochim. Acta*, 235 (2017) 72–78.
- [6] S. Pandey, A comprehensive review on recent developments in bentonite-based materials used as adsorbents for wastewater treatment, *J. Mol. Liq.*, 241 (2017) 1091–1113.
- [7] S. Daneshfozoun, M.A. Abdullah, B. Abdullah, Preparation and characterization of magnetic biosorbent based on oil palm empty fruit bunch fibers, cellulose and *Ceiba pentandra* for heavy metal ions removal, *Ind. Crop. Prod.*, 105 (2017) 93–103.
- [8] M. Afzaal, B. Periyasamy, M.A. Abdullah, Continuous heavy metal removal from palm oil mill effluent using natural *Ceiba pentandra* (L.) Gaertn packed-bed column. *Appl. Mech. Mater.*, 625 (2014) 822–825.
- [9] R. Malik, S. Dahiya, S. Iata, An experimental and quantum chemical study of removal of utmostly quantified heavy metals in wastewater using coconut husk: A novel approach to mechanism, *Int. J. Biol. Macromol.*, 98 (2017) 139–149.
- [10] C. Mânzatu, B. Nagy, C. Majdik, The biosorptive effect of untreated and chemically modified fir cone powder on Pb (II) removal, *Eur. J. Wood. Wood. Prod.*, 75 (2017) 623–632.
- [11] A. Ali, Removal of Mn (II) from water using chemically modified banana peels as efficient adsorbent, *Environ. Nano technol. Monitor. Manag.*, 7 (2017) 57–63.
- [12] N. Gupta, R. Sen, Kinetic and equilibrium modelling of Cu (II) adsorption from aqueous solution by chemically modified groundnut husk (*Arachis hypogaea*), *J. Environ. Chem. Eng.*, 5 (2017) 4274–4281.
- [13] D. Mohammed, R. Hashim, M. Rafatullah, O. Sulaiman, A. Ahmad, Adsorption of Pb (II) ions from aqueous solutions by date bead carbon activated with ZnCl<sub>2</sub>, *Clean-Soil, Air, Water*, 39 (2011) 392–399.
- [14] J. Singh, N. Dhiman, N.K. Sharma, Effect of Fe (II) on the adsorption of Mn (II) from aqueous solution using esterified saw dust: equilibrium and thermodynamic studies, *Indian Chem. Eng.*, (2017) 1–14.
- [15] M.I. Errea, E. Rossi, S.N. Goyanes, N.B. D'Accorso, Chitosan: From organic pollutants to high-value polymeric materials, In: S.N. Goyanes, N.B. D'Accorso, *Industrial Applications of Renewable Biomass Products: Past, Present and Future*, Springer International Publishing, Cham, 2017, pp. 251–264.
- [16] Q. Liu, J.J. Schauer, Local-acting air pollutant emissions from road vehicles, In: *Environmental impacts of road vehicles: past, present and future*, The Royal Society of Chemistry, 2017, pp. 46–85.
- [17] G. Marsh, N. Hill, J. Sully, Consultation on the need to reduce the sulphur content of petrol and diesel fuels below 50 ppm :- A policy makers summary, A report produced for the European Commission DG Environment, AEAT/ENV/R/0372 Issue 5, 2000, pp. 1–107.
- [18] S.W. Lee, J.W. Ryu, W.Min, SK Hydrodesulfurization (HDS) pretreatment technology for ultra low sulfur diesel (ULSD) production, *Catal. Surveys Asia*, 7 (2003), pp. 271–279.
- [19] M. Ergorova, Study of aspects of deep hydrodesulphurization by means of model reactions, Doctoral Thesis, Swiss Federal Institute of Technology, Zurich, 2003.
- [20] M.M. Ramirez-Corredores, Z. Hernandez, J. Guerra, R.V. Navarro, Selective sulfur removal from hydrocarbon streams by absorption US Patent, US7446077 B2, 2008.
- [21] I. Siró, D. Plackett, Micro fibrillated cellulose and new nano composite materials: a review, *Cellulose*, 17 (2010) 459–494.
- [22] R.M. Rowell, Paper and composites from agro-based resources, CRC Press, University of Wisconsin, Madison, USA; Judith Rowell, USDA, Madison, WI, 1996.
- [23] D.W. O'Connell, C. Birkinshaw, T.F. O'Dwyer, Heavy metal adsorbents prepared from the modification of cellulose: A review, *Bioresour. Technol.*, 99 (2008) 6709–6724.
- [24] S. Daneshfozoun, B. Abdullah, M.A. Abdullah, Heavy metal removal by Oil Palm Empty Fruit Bunches (OPEFB) biosorbent. *Appl. Mech. Mater.*, 625 (2014) 889–892.
- [25] M.S. Nazir, B.A. Wahjoedi, A.W. Yussof, M.A. Abdullah, Eco-friendly extraction and characterization of cellulose from oil palm empty fruit bunches, *BioResour.*, 8 (2013) 2161–2172.
- [26] M.A. Abdullah, M.S. Nazir, M.R. Raza, B.A. Wahjoedi, A.W. Yussof, Autoclave and ultra-sonication treatments of oil palm empty fruit bunch fibers for cellulose extraction and its polypropylene composite properties, *J Clean Prod.*, 126 (2016) 686–697.
- [27] TAPPI, Alpha-, beta- and gamma- cellulose in pulp. In: *Fibrous material and pulp testing*, T 203 om 88, Atlanta, TAPPI Press, 1991.
- [28] ASTM, Annual Book of ASTM Standard, In: *Soap, Polishes cellulose leather, Resilient Floor covering*, 15, 1983.
- [29] C. Yun, X. Xiao-peng, Y. Guang, Z. Li-na, L. Se-lin, L. Hui, Characterization of regenerated cellulose membranes hydrolyzed from cellulose acetate, *Chinese J. Polym. Sci.*, 20 (2002) 369–375.
- [30] S. Lagergren, About the theory of so-called adsorption of soluble substances, *Kungliga Svenska Vetenskapsakademiens Handlingar*, 24 (1898) 1–39.
- [31] Y.S. Ho, W.T. Chiu, C.C. Wang, Regression analysis for the sorption isotherms of basic dyes on sugarcane dust, *Bioresour. Technol.*, 96 (2005) 1285–1291.
- [32] S. Karagöz, T. Tay, S. Ucar, M. Erdem, Activated carbons from waste biomass by sulfuric acid activation and their use on methylene blue adsorption, *Bioresour. Technol.*, 99 (2008) 6214–6222.
- [33] M.J. Temkin, V. Pyzhev, Recent modification to Langmuir isotherm, *Acta. Physiochim. U.S.S.R.*, 12 (1940) 217–222.
- [34] M.M.L. Loo, R. Hashim, C.P. Leh, Recycling of valueless paper dust to a low grade cellulose acetate: Effect of pretreatments on acetylation, *BioResour.*, 7 (2012) 1068–1083.
- [35] M.S. Rosnah, A.A. Astimar, W. Hasamudin, W. Hassan, M.T. Gapor, Solid-state characteristics of micro crystalline cellulose from oil palm empty fruit bunch fibre, *J. Oil Palm Res.*, 21 (2009) 613–620.
- [36] F. Fahma, S. Iwamoto, N. Hori, T. Iwata, A. Takemura, Isolation, preparation, and characterization of nano fibers from oil palm empty-fruit-bunch (OPEFB), *Cellulose*, 17 (2010) 977–985.
- [37] Y. Tian, M. Wu, R. Liu, D. Wang, X. Lin, W. Liu, L. Ma, Y. Li, Y. Huang, Modified native cellulose fibers—A novel efficient adsorbent for both fluoride and arsenic, *J. Hazard. Mater.*, 185 (2011) 93–100.
- [38] M.J. Haron, M. Tiansin, N.A. Ibrahim, A. Kassim, W.M. Wan Yunus, S.M. Talebi, Sorption of Pb (II) by poly(hydroxamic acid) grafted oil palm empty fruit bunch, *Water Sci. Technol.*, 63 (2011) 1788–1793.
- [39] M.N.M. Ibrahim, W.S.W. Ngah, M.S. Norliyana, W.R.W. Daud, M. Rafatullah, O. Sulaiman, R. Hashim, A novel agricultural waste adsorbent for the removal of lead (II) ions from aqueous solutions, *J. Hazard. Mater.*, 182 (2010) 377–385.
- [40] J.T. Matheickal, Q. Yu, Biosorption of lead (II) and copper (II) from aqueous solutions by pre-treated biomass of Australian marine algae, *Bioresour. Technol.*, 69 (1999) 223–229.
- [41] O.K. Júnior, L.V.A. Gurgel, R.P. de Freitas, L.F. Gil, Adsorption of Cu (II), Cd (II), and Pb (II) from aqueous single metal solutions by mercerized cellulose and mercerized sugarcane bagasse chemically modified with EDTA dianhydride (EDTAD), *Carbohydr. Polym.*, 77 (2009) 643–650.
- [42] Y.S. Ho, W.T. Chiu, C.S. Hsu, C.T. Huang, Sorption of lead ions from aqueous solution using tree fern as a sorbent, *Hydro metallurgy*, 73 (2004) 55–61.
- [43] N. Jafari, Z. Senobari, Removal of Pb (II) ions from aqueous solutions by *Cladophora rivularis* (Linnaeus) Hoek, *Sci. World J.*, 2012 (2012) 6.
- [44] R.F. Carbonaro, Y.B. Atalay, D.M. Di Toro, Linear free energy relationships for metal-ligand complexation: Bidentate binding to negatively-charged oxygen donor atoms, *Acta Cosmochim. Geochim.*, 75 (2011) 2499–2511.
- [45] L.D. Hafshejani, S.B. Nasab, R.M. Gholami, M. Moradzadeh, Z. Izadpanah, S.B. Hafshejani, A. Bhatnagar, Removal of zinc and lead from aqueous solution by nano structured cedar leaf ash as biosorbent, *J. Mol. Liq.*, 211 (2015) 448–456.

- [46] P. Gao, Y. Feng, Z. Zhang, C. Wang, J. Liu, N. Ren, Kinetic and thermodynamic studies of phenolic compounds' adsorption on river sediment, *Soil Sediment Contaminat. Int. J.*, 21 (2012) 625–639.
- [47] S. Daneshfozoun, Heavy metal ions removal using magnetic bio-sorbent based on agro-lignocellulosic materials, PhD Thesis, Universiti Teknologi PETRONAS, 2017.
- [48] C. Moreno-Castilla, Adsorption of organic molecules from aqueous solutions on carbon materials, *Carbon*, 42 (2004) 83–94.
- [49] Q.S. Liu, T. Zheng, P. Wang, J.P. Jiang, N. Li, Adsorption isotherm, kinetic and mechanism studies of some substituted phenols on activated carbon fibers, *Chem. Eng. J.*, 157 (2010) 348–356.
- [50] E. Maekawa, T. Koshijima, Preparation and characterization of hydroxamic acid derivative and its metal complexes derived from cellulose, *J. Appl. Polym. Sci.*, 40 (1990) 1601–1613.
- [51] K.S. Low, C.K. Lee, S.M. Mak, Sorption of copper and lead by citric acid modified wood, *Wood Sci Technol.*, 38 (2004) 629–640.
- [52] H. Liu, F. Zhang, W. Li, X. Zhang, C.S. Lee, W. Wang, Porous tremella-like  $\text{MoS}_2$ /polyaniline hybrid composite with enhanced performance for lithium-ion battery anodes, *Electrochim. Acta.*, 167 (2015) 132–138.
- [53] Y. Xia, Y. Li, Y. Gu, T. Jin, Q. Yang, J. Hu, H. Liu, H. Wang, Adsorption desulfurization by hierarchical porous organic polymer of poly-methylbenzene with metal impregnation, *Fuel*, 170 (2016) 100–106.
- [54] J.A. Arcibar-Orozco, J.R. Rangel-Mendez, Model diesel denitrogenation by modified activated carbon with iron nano particles: Sulfur compounds effect, *Chem. Eng. J.*, 230 (2013) 439–446.
- [55] M.A. Abdullah, A.U. Rahmah, Z. Man, Physicochemical and sorption characteristics of Malaysian *Ceiba pentandra* (L.) Gaertn. as a natural oil sorbent, *J. Hazard. Mater.*, 177 (2010) 683–691.
- [56] M.A. Abdullah, M. Afzaal, Z. Ismail, A. Ahmad, M.S. Nazir, A.H. Bhat, Comparative study on structural modification of *Ceiba pentandra* for oil sorption and palm oil mill effluent treatment, *Desalin. Water Treat.*, 54 (2015) 3044–3053.
- [57] M.A. Abdullah, S.H. Gheewala and A. Ullah, Integrated biorefinery and life-cycle analysis for sustainable production of biofuels and bioproducts based on microalgal cultivation and palm oil milling, In: Proceeding of the 13<sup>th</sup> Universiti Malaysia Terengganu International Annual Symposium on Sustainability Science and Management: Science and Technology for Sustainable Livelihood, Primula Beach Hotel, Kuala Terengganu, Terengganu, Malaysia, UMTAS 2016140, 13-15th December, pp. 319–322, 2016.
- [58] M.A. Abdullah, M.S. Nazir, H. Ajab, S. Daneshfozoun, S. Almstapha, Advances in eco-friendly pre-treatment methods and utilization of agro-based lignocelluloses. In: D. Thangadurai and J. Sangeetha, *Industrial Biotechnology: Sustainable Production and Bioresource Utilization*, Apple Academic Press, USA, 2017, pp 371–420.